

# Motor bearing damage detection using Radar

**PROBLEM:** Is possible to determine the health status of the motor using non-contact sensors and non-destructive testing

# State of art (summary):

**KEY CONCEPT:** Each fault is related to a precise harmonic in the spectrum

## 1) MCSA(motor current signature analysis)

This method require to measure the variation of the absorbed current from the motor.

From the current spectra is able to identify motor's fault thanks to a specific relationship.

## 2) Vibration analysis

Usually It is based on 3-axis MEMS accelerometers that measure the vibration of the shaft. Also in this case is possible to find fault analysing the spectrum of the displacement of the shaft.

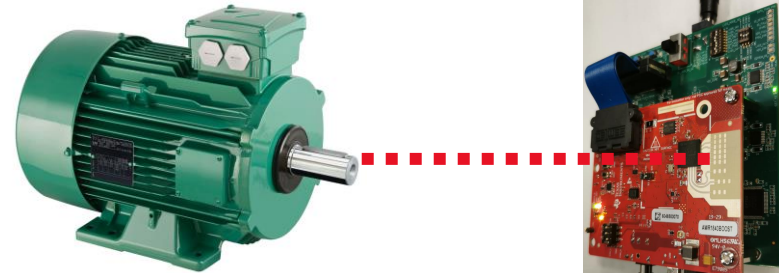
<b>MCSA</b>	<b>Vibration analysis</b>	<b>Vibration analysis with Lidar/Radar</b>
non-invasive	independent of the type of motor power supply	independent of the type of motor power supply
Easy to implement	low power consumption	High reliability
low signal-to-noise ratio	Low reliability	Non contact-sensors
contact-sensors	contact-sensors	High cost

# Project's aim

The aim is to determine the health status of the motor  
developing the vibration analysis with a Radar



The project want to demonstrate if its possible to use a radar  
for detecting shaft's vibration

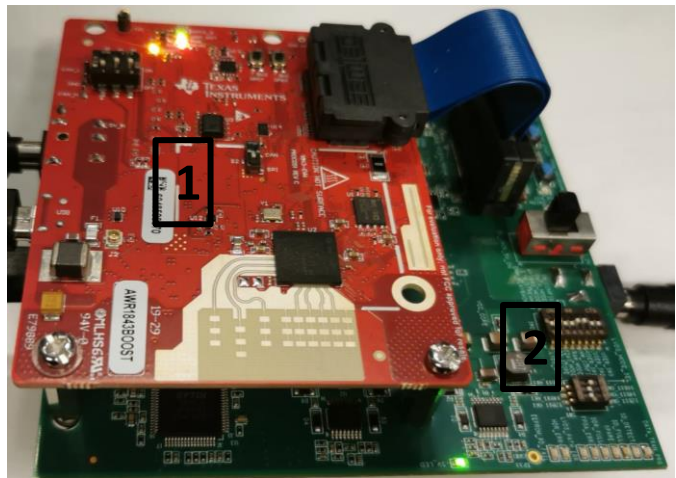


## **Assumptions:**

- 1) Only inner race bearings defect has been considered
- 2) Only air between the Radar and the target
- 3) Consider only one direction vibration

Processing & plotting

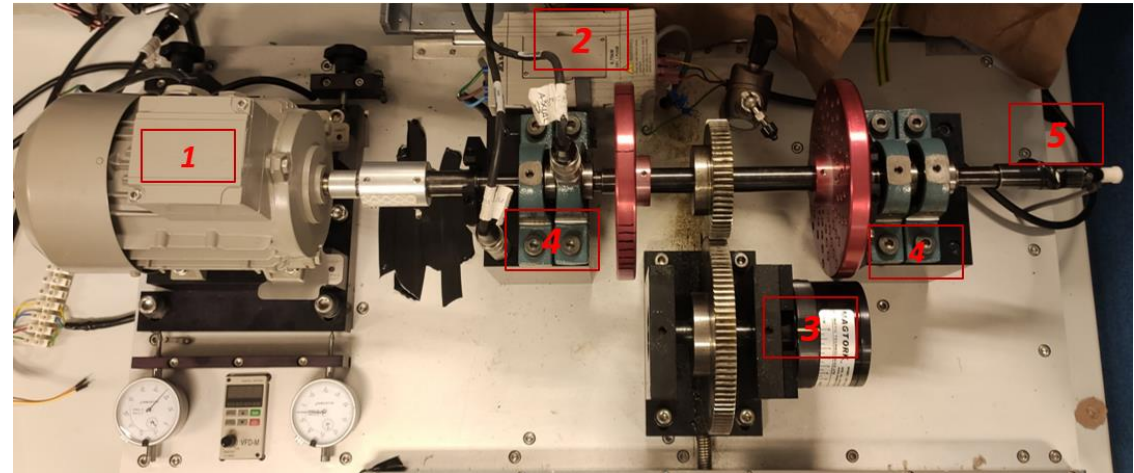
# Experimental setup:



1. Radar T.I.-AWR1843
2. Capture Card T.I. DCA1000EVM



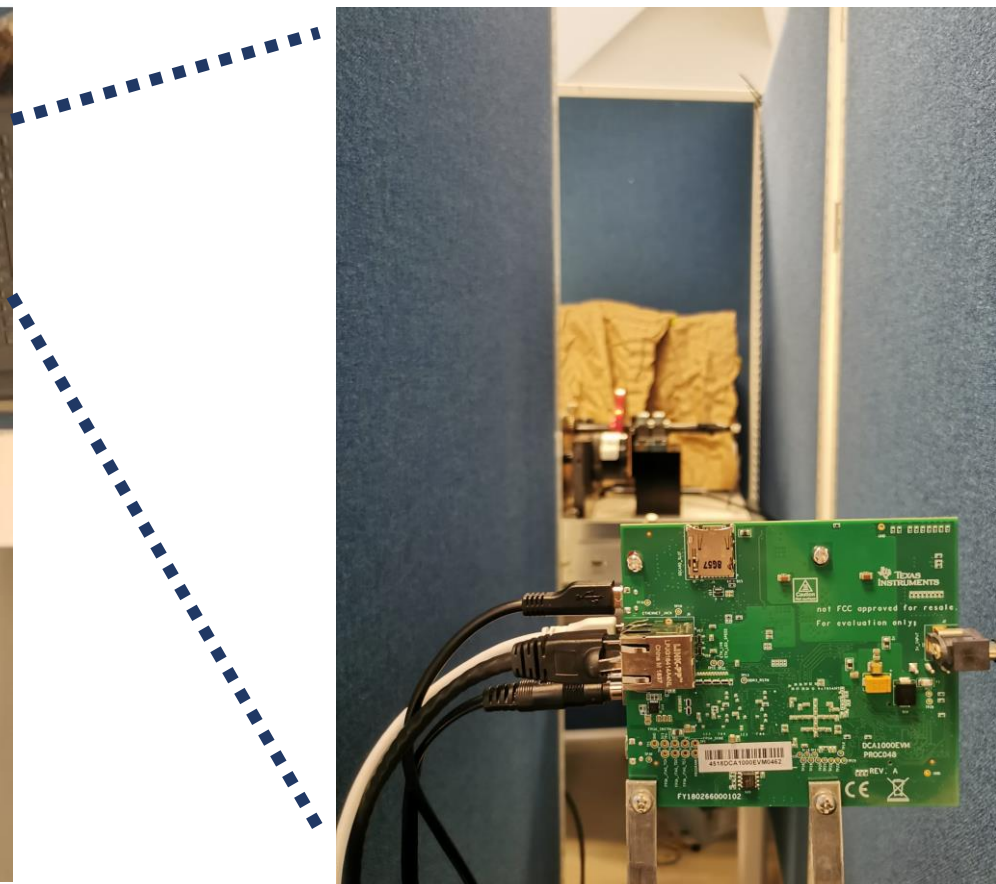
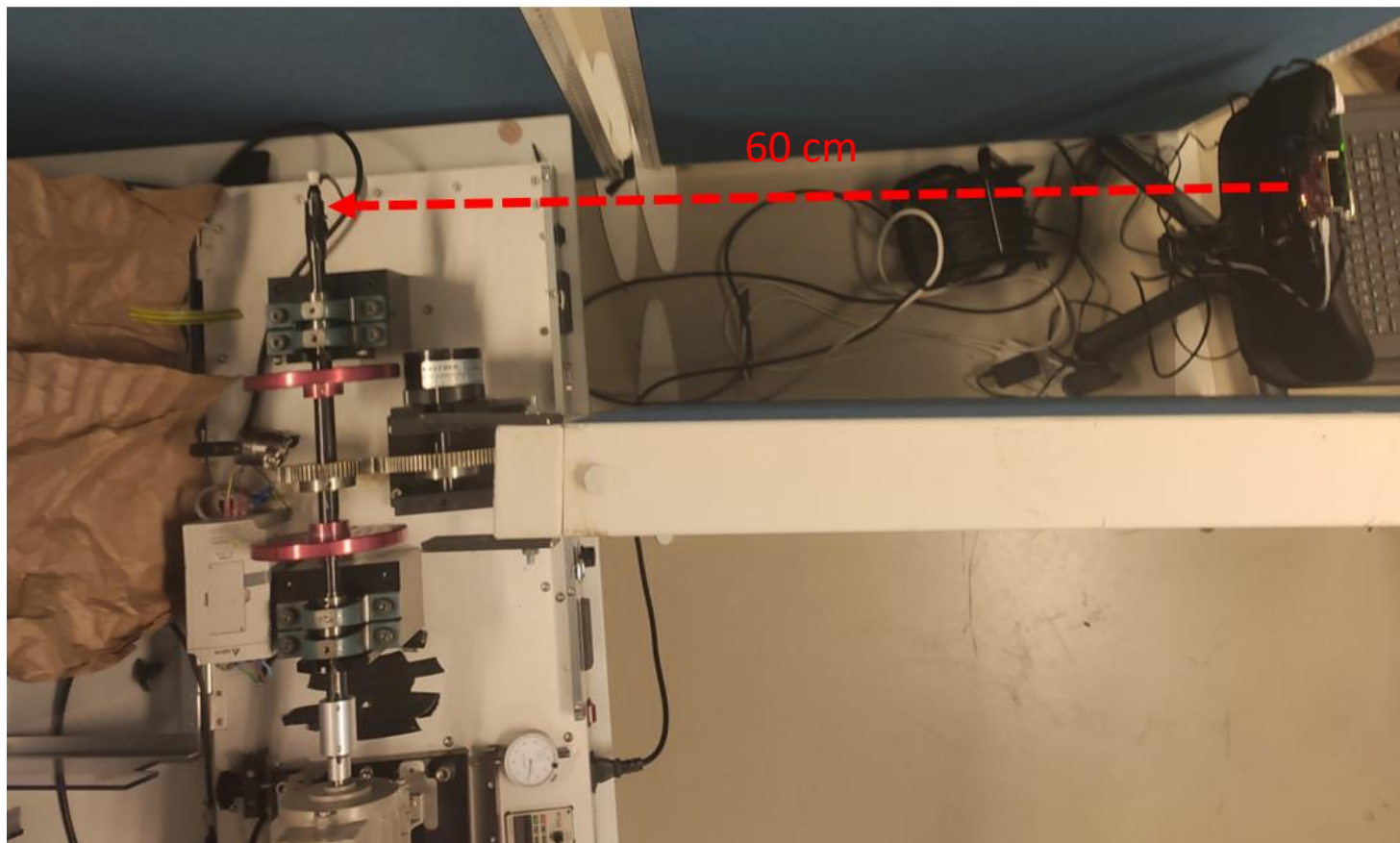
mmWaveStudio 2.0 Software



1. Siemens 0.37 KW IM
2. VFD-M
3. Magnetic Brake
4. Bearings
5. Measuring Point

Frequency	50 Hz	60 Hz	
Rated motor power	0.37 kW	0.43 kW	
Rated motor speed	1370 1/min	1669 1/min	
Rated motor torque	2.6 Nm	2.5 Nm	
Rated motor current (IE) :	VD 1.84 A	VY 1.06 A	
Starting- / rated motor current	3.3	3.8	
Breakdown / rated motor	2,1	2,2	
Starting- / rated motor torque	1.9	2.0	
Efficiency %	4/4 65,8%	3/4 64,8%	2/4 60,8%
Power factor	0,78	0,72	0,61
Efficiency class /	-/-	-/-	0,58

# Experimental setup:



# Study cases:

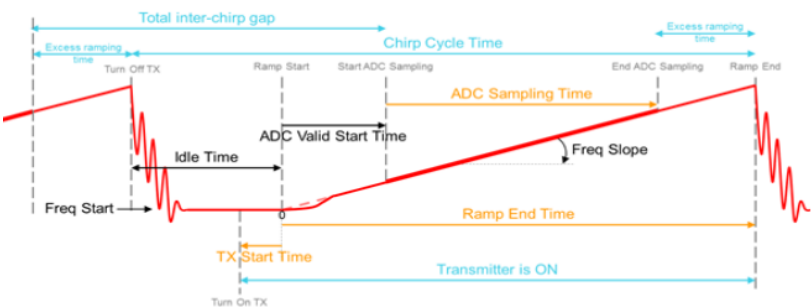
1) Stationary

2) Healthy bearings:

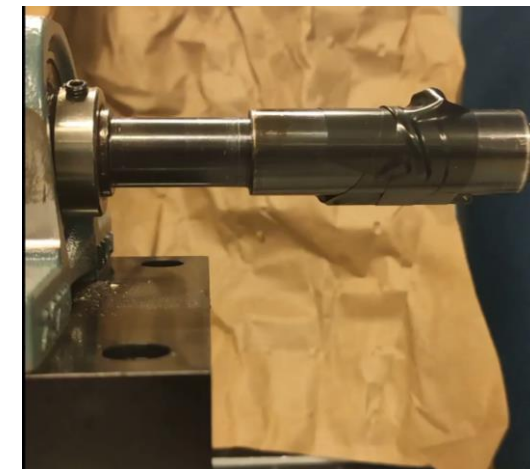
- i. 5 [Hz]
- ii. 15 [Hz]
- iii. 25 [Hz]

3) Faulty bearing:

- i. 5 [Hz]
- ii. 15 [Hz]
- iii. 25 [Hz]



Good



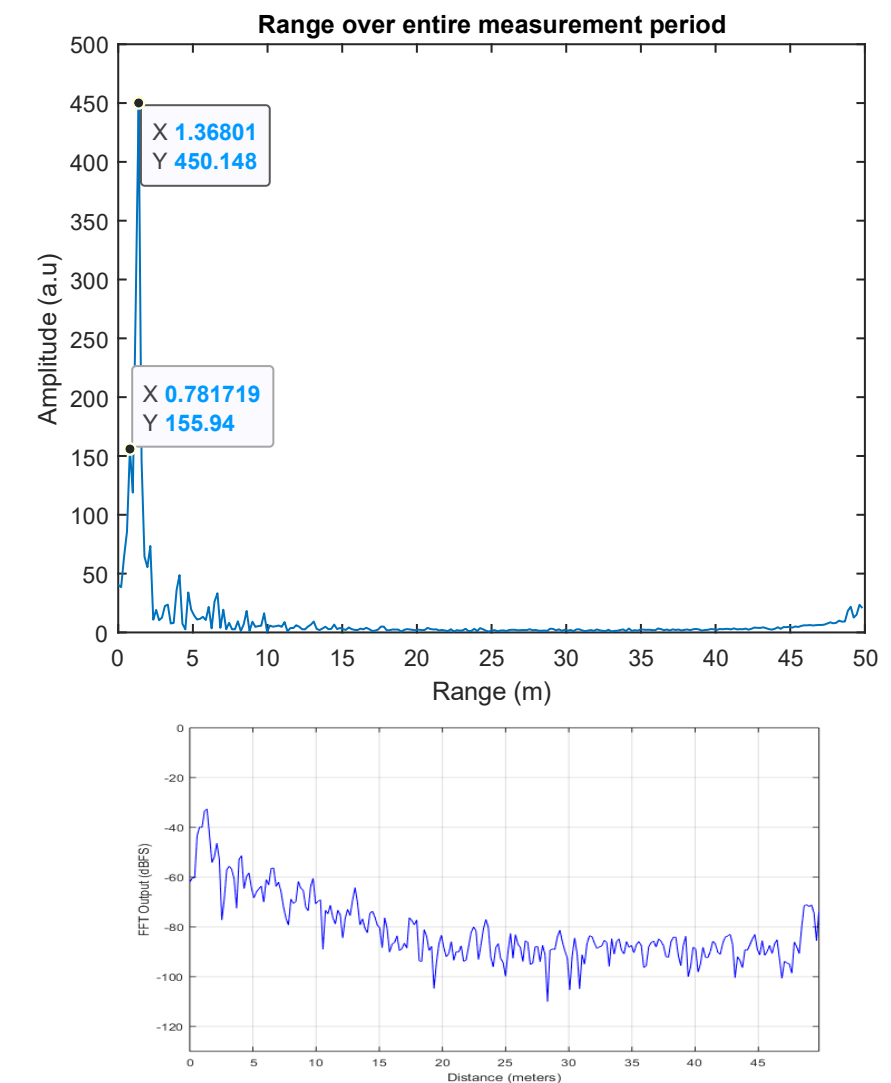
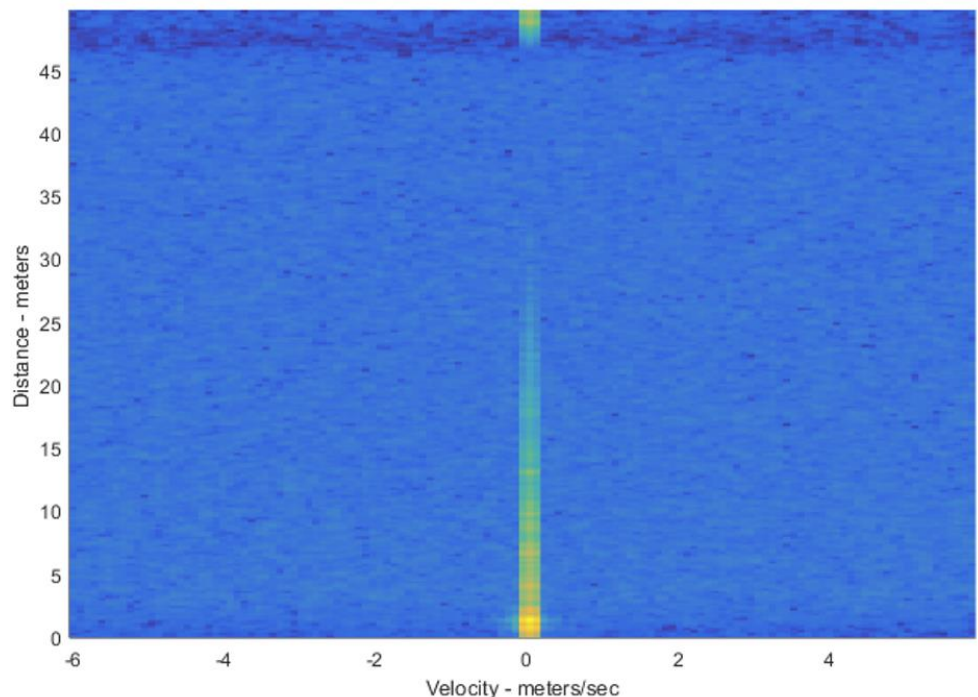
Faulty

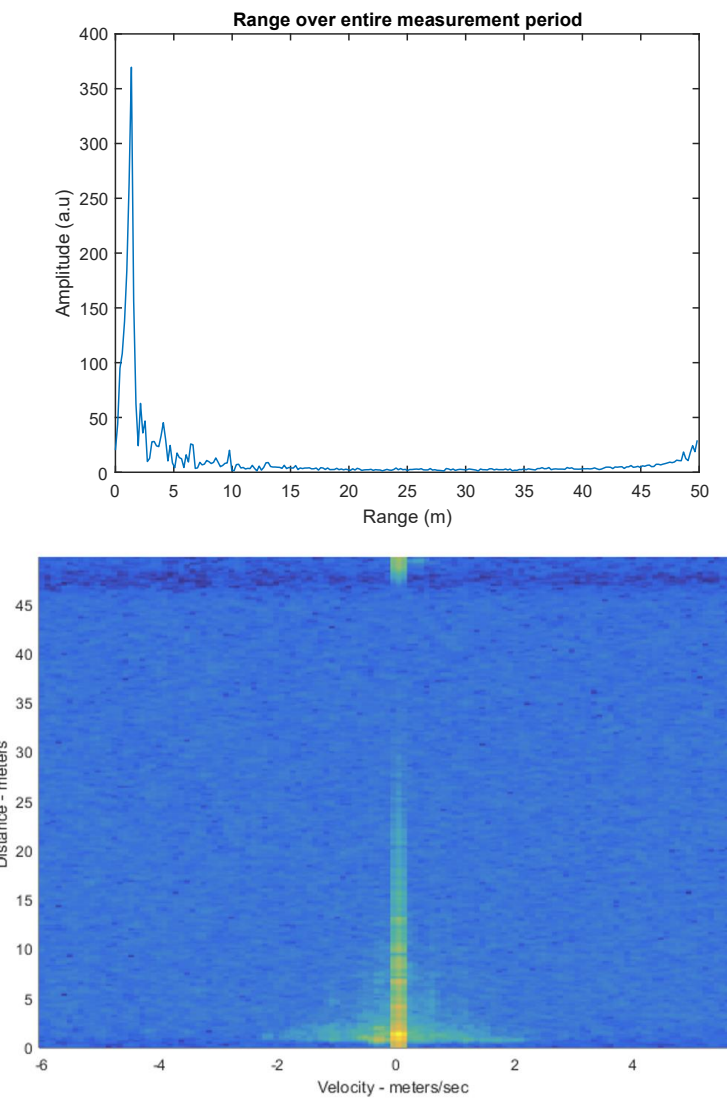
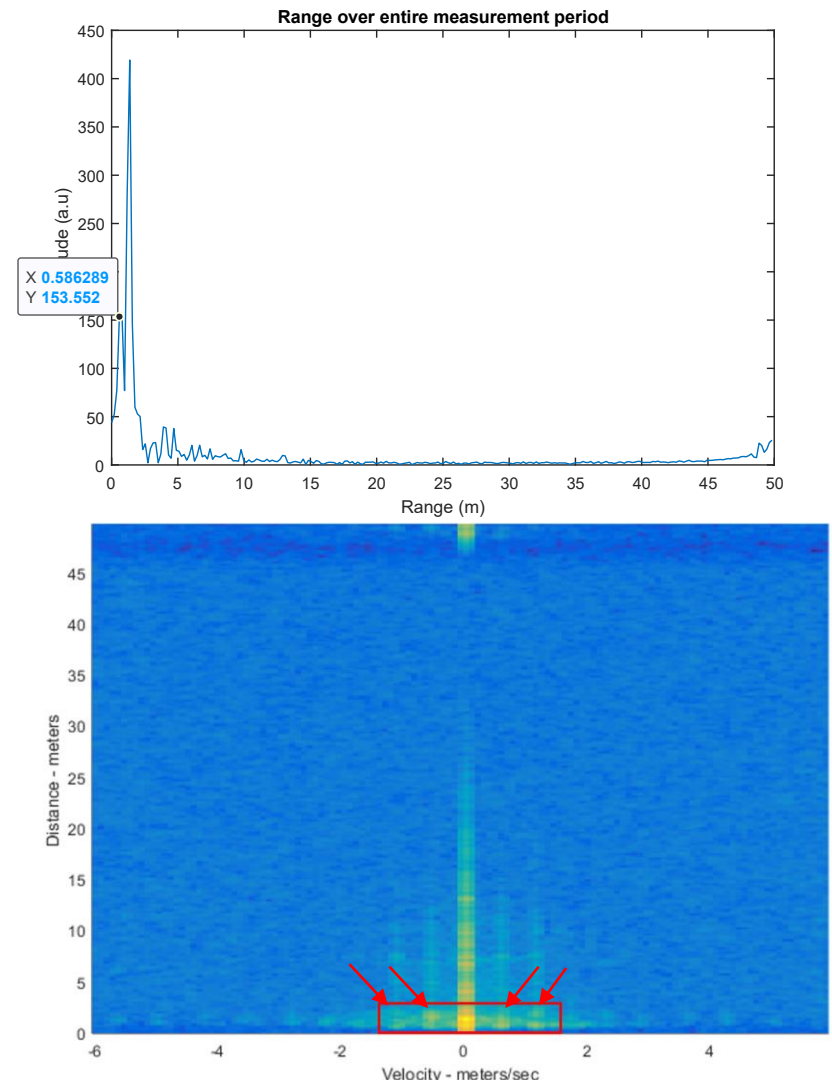


## PARAMETERS

- 128 chirps per frame
- 40ms frame periodicity
- 77GHz start frequency
- 29,982 frequency slope
- 256 ADC samples

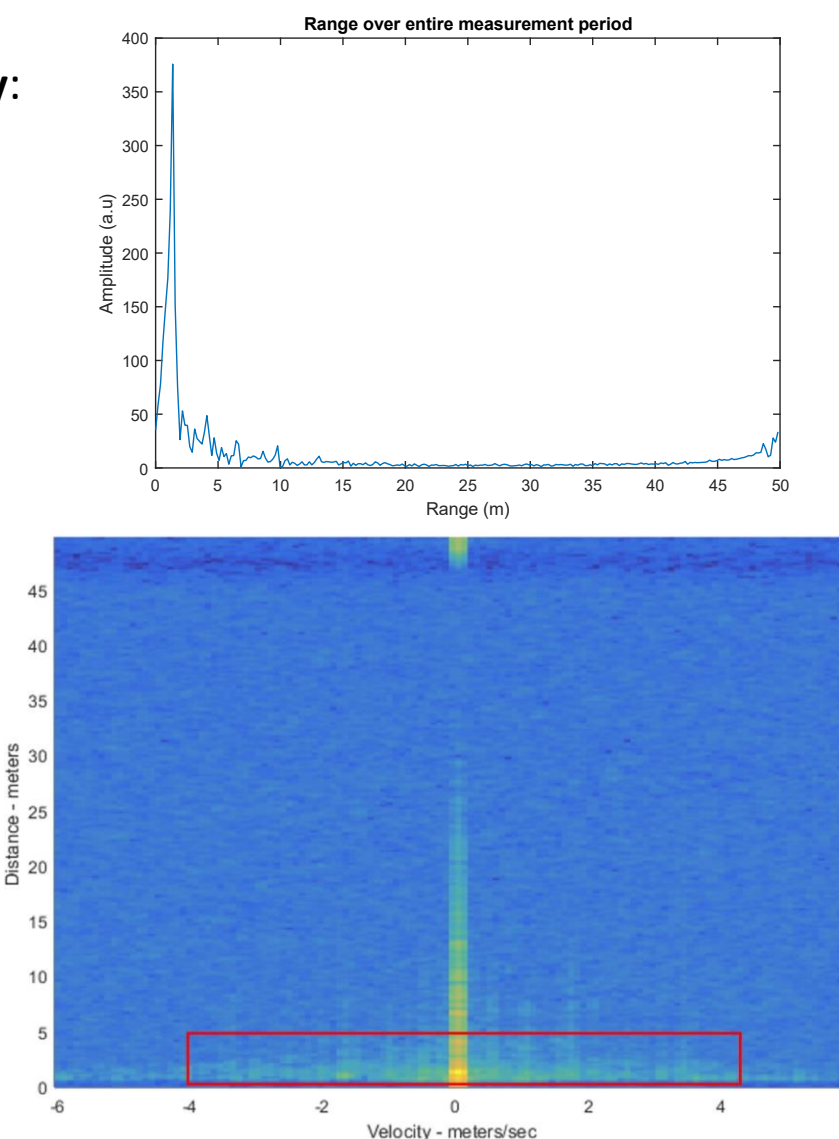
# 1)Stationary:



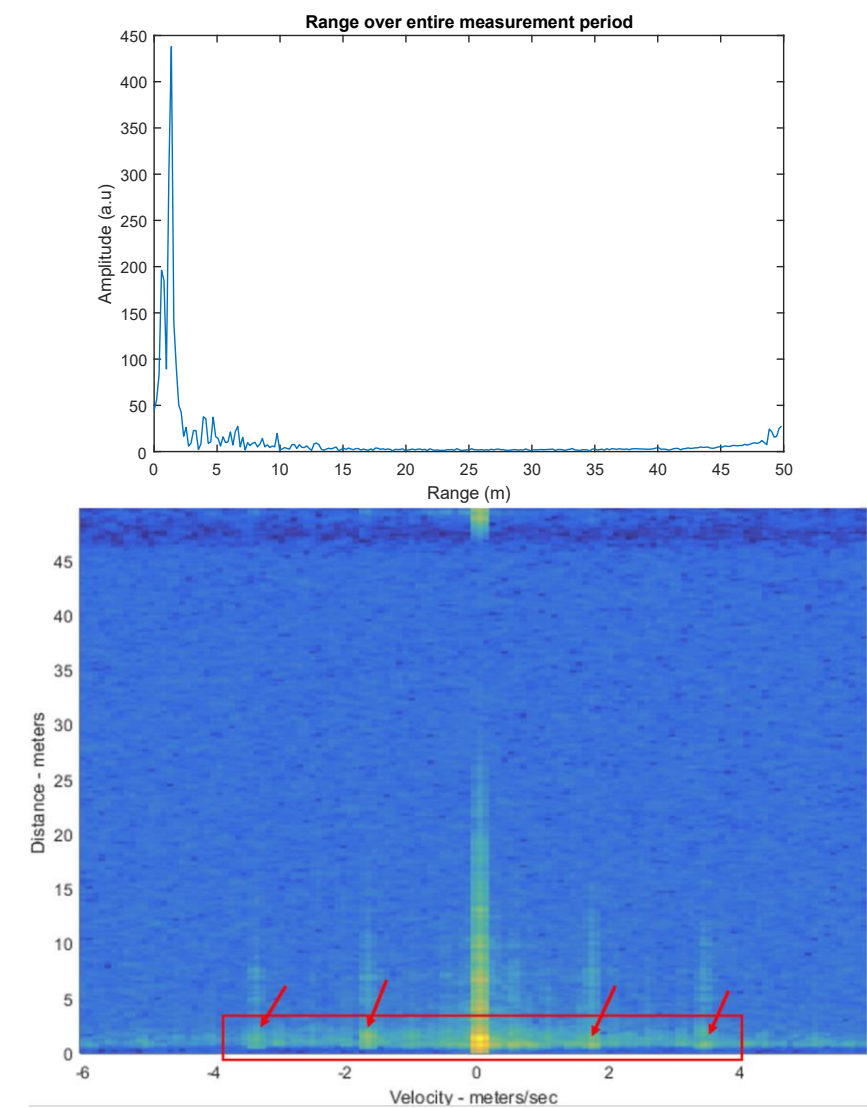
**Healthy:****Faulty:**

# 15Hz:

**Healthy:**

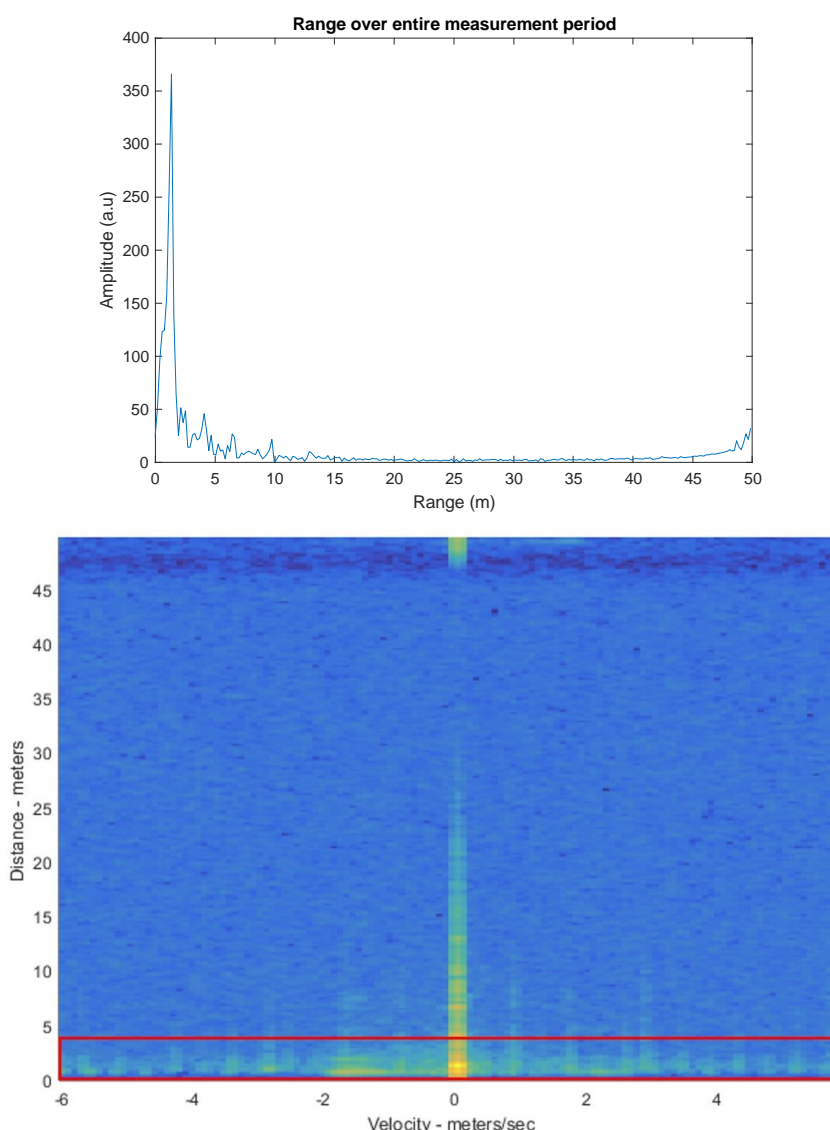


**Faulty:**

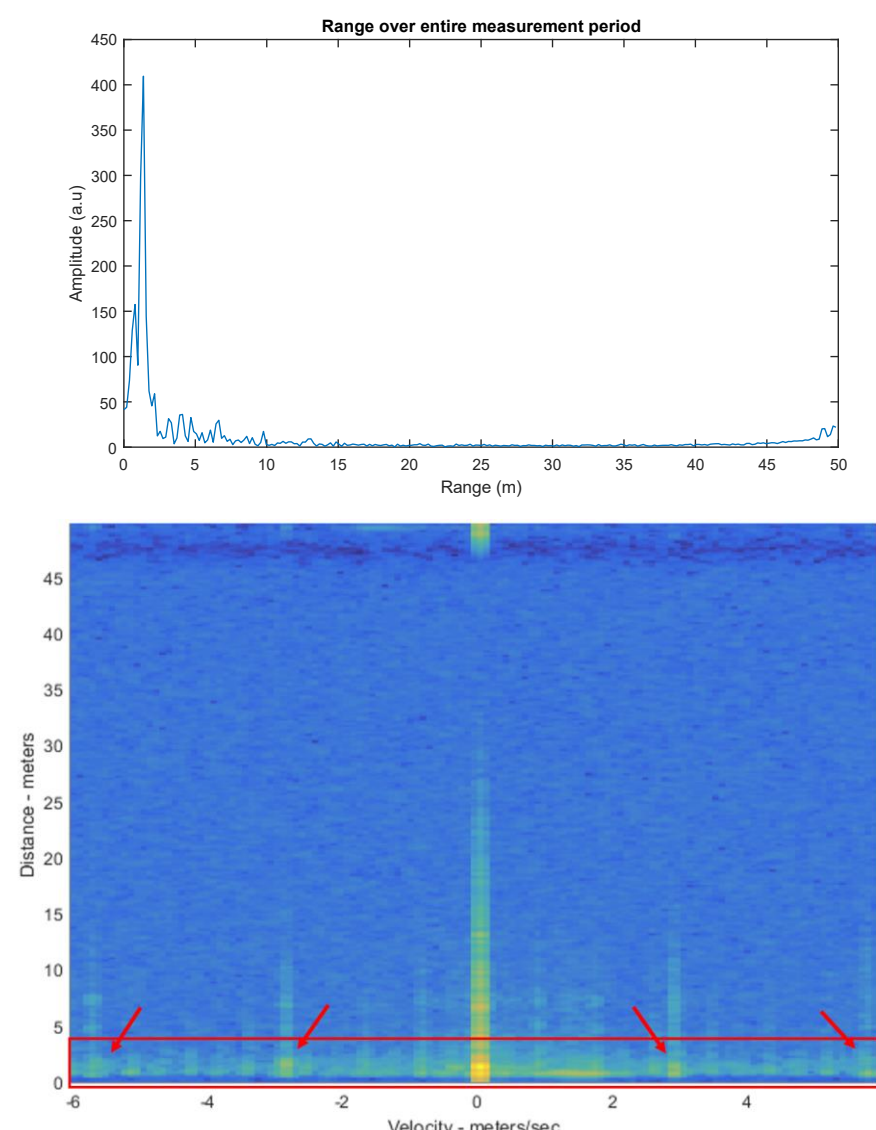


# 25Hz:

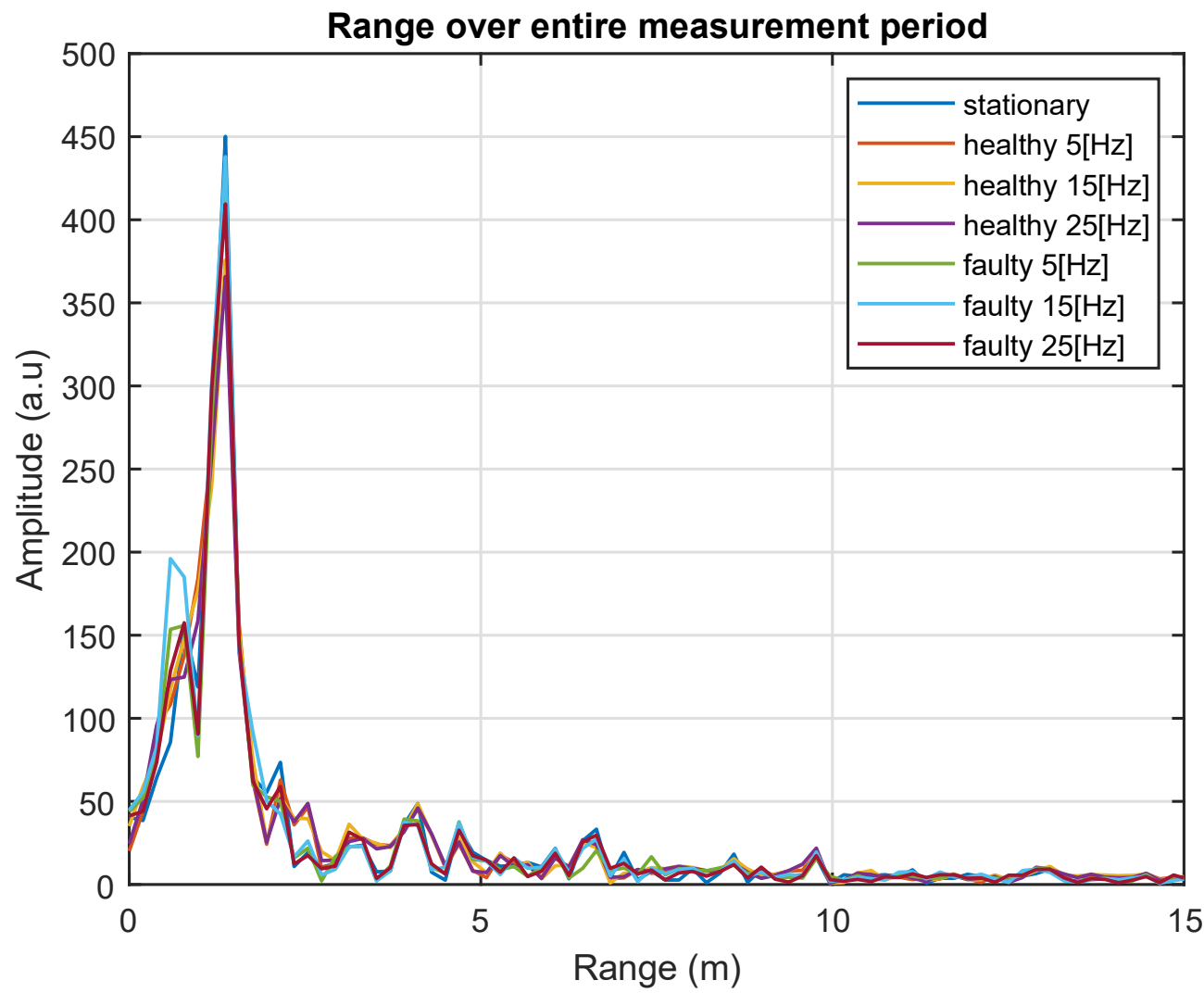
**Healthy:**



**Faulty:**



# Final results:



# To sum up:

Is possible to detect the vibration of the shaft using a radar, in particular can detect the 1<sup>st</sup> and 2<sup>nd</sup> harmonics at low frequency. Because the radar has a low resolution in range and speed but also our setup has a slow ADC that cannot acquire a lot of sample for each frame.

Using a Lidar, which has a better resolution could be possible to detect vibration also at high frequency and also higher harmonics.

Thanks for the attention!

# Motor bearing damage detection using Radar

Gianluca Salata

**Abstract**—This paper addresses the application of a non contact sensor for the detection of rolling-element bearing damage in induction machines; in particular using a Radar to detect vibration of motor's shaft. Vibration monitoring of mechanical bearing frequencies is currently used to detect the presence of a fault condition. Since these mechanical vibrations are associated with damage in the inner race defects of the bearings, the outer race defects is modulated and ball defects are generated at predictable frequencies related to bearings geometry and operating speed.

This paper takes the initial step of investigating the efficacy of using a radar for shaft's vibration caused by a inner race faulty bearing, in particular by correlating the relationship between vibration and the range doppler data of a radar. The aim of the paper is to define if is possible to acquire vibration data of a shaft with a radar and its limits. This can help to improve the classical vibration analysis, modifying the sensing part using a non contact sensor.

## I. INTRODUCTION

NOWADAYS, timely maintenance of electric motors is vital to keep up the complex processes of industrial production. One of the most common cause of motor failures is bearing faults. Early detection of this faults allows replacement of the components, rather than replacement of the motor. Determine the continuous health of a motor can be useful to predict a failure and to enable some procedures to put the motor into safety condition. This can also help the engineer to be aware of the type of the failure that occur. Analysing the behaviour of a motor is possible to discover an incoming fault in it. There is a strong relationship between the type of fault and some variable parameters of the motor, such as the input current or the shaft vibration. Modern technique exploit this relation to detect the fault, each of them with advantages and disadvantages but all of them rely on contact sensors. Motors are usually placed in hostile environments, in particular induction motors, so the sensor need to be rugged and designed to survive for a long period of time at critic condition. With this paper, the aim is to overcome the problem to place a sensor in contact with the motor when it is located in hostile or not very accessible environments. A radar is potentially able to detect a vibration of a motor from distance, for example from a more accessible and safer place instead being in the same area of the motor; this could improve the lifespan of the sensor and the maintainability of the sensing system. This paper demonstrate how to acquire data from a non contact sensor such a radar in order to use them in the vibration analysis for detection of two different bearing fault: inner and outer race bearing's defect fault.

G. Salata was with the faculty of Engineering and Science Universitetet i Agder, Grimstad, 4078 NOR

Ajit Jha are with University of Agder .

Manuscript made November 10, 2021; revised November 10, 2021

## II. STATE OF ART

Different methods were being proposed in order to overcome the problem with the most common technique and to improve the reliability of the system; Paulo and Daniel, in [1] proposed to detect fault through sound and vibration signals; in fact the sound is a physical phenomenon that provides information about the behaviour of a system and can be used as a parameter for determining the condition thereof. The acoustic sound waves contain information about the health status of the machine because sound is produced by mechanical vibrations. The electric motor is not an exception, and the vibrations generated by defects in bearings, mechanical unbalances and broken rotor bars produce sounds with characteristic frequencies associated with each fault. However the downside of sound signal analysis is its sensitivity to external noise , which should be avoided whenever possible; this limits enormously the application of this technique. The diagnosis through the analysis of acoustic sound signal is a first non-invasive method using non-contact sensor, a microphone in this case, to check the motor's status.

Kim, Dong-Yeon [2] demonstrates that is possible to detect the health status of bearings, for example inside of a motor, using infrared thermography camera, so using a non-contact sensor and non-destructive. This method, called infrared thermography, can evaluate precisely the temperature characteristics according to the condition of the ball bearing because a fault inside of a bearing corresponds to friction that generates heat. It is based on the temperature distribution and thermal changes inside of the motor, in particular looking at the bearing. This method is very reliable and its very accurate for detecting the presence of a fault but it cant determine which type of fault occur inside of the bearing, because it is based only on the thermal map of the bearing. The presence of lubricant inside prevents from detecting the source of heat, corrupting the thermal image, so its more complicated detect the origin of the fault.

The most popular and used technique for the detection of faults in induction motors with contact sensors are: the MCSA (motor current signature analysis) and the analysis of vibration signals. Both methods are based on the same concept: each fault is related to a precise harmonic component. It means that from a Fourier transform of a signal is possible to determine the which fault occur inside the motor. They differ in the signal they analyse: MCSA use the supplying current signal while vibration analysis is based on the displacement of motor's shaft.

### A. MCSA

This technique involves the analysis of stator current signals collected with a current clamp or an ammeter. It is based on

the recognition that an electric motor (ac or dc) driving a mechanical load acts as an efficient and permanently available transducer by sensing mechanical load variations and converting them into variations in the induced current generated in the motor windings. These motor current variations are carried by the electrical cables processes as desired. Motor current signatures, obtained in both time and over time to provide early indication of degradation. As described in [3], to diagnose motor faults, MCSA uses the current spectra, which contains potential information of motor faults. Therefore, it is important that abnormal harmonic frequencies are independent of the types of drive-systems or control techniques. [4] and [5] relate each bearing fault to a precise harmonic in the current spectra, using the geometry of the bearing; for example a bearing failure cause the variation of air-gap length when a rotor turns and it generates a harmonic at the frequency:

$$f_{bearing} = f_0 \pm n_b f_{i,0} \quad (1)$$

$$f_{i,0} = \frac{n}{2} (1 - s) f_0 \left\{ 1 \pm \frac{BD}{PD} \cos \beta \right\} \quad (2)$$

Where  $n_b$  is the number of balls,  $PD$  is the bearing-pitch diameter,  $BD$  is the ball diameter,  $\beta$  is the contact angle of crack on races, and  $n$  is the positive integer,  $f_0$  is the electrical supply frequency,  $s$  is the per-unit slip respectively. In MCSA, the equation to determine the harmonic's frequency of bearing fault are almost similar to the equation in the vibration analysis; to obtain the frequency in MCSA is necessary to add the supply frequency of the motor to the equation of vibration analysis. The MCSA technique has the advantages of being non-invasive, easy and cheap to implement, providing good results in fault diagnosis; however, under certain conditions its application is not sensitive enough because it has a low signal-to-noise ratio.

### B. Vibration analysis

It is based on the signal coming from accelerometers/vibrometers positioned on the crankshaft; 3-axis MEMS accelerometers are frequently used due to its ability to measure vibration at very low frequency, around 0Hz. The bearing fault related vibration frequencies are easily calculated with known bearing geometry and rotor speed as explained in [6]. The equation to determine the frequency for each type of bearing's defect are:

$$f_{OD} = \frac{n}{2} f_{rm} \left( 1 - \frac{BD}{PD} \cos \phi \right) \quad (3)$$

$$f_{ID} = \frac{n}{2} f_{rm} \left( 1 + \frac{BD}{PD} \cos \phi \right) \quad (4)$$

$$f_{BD} = \frac{PD}{2BD} f_{rm} \left( 1 - \left( \frac{BD}{PD} \right)^2 \cos^2 \phi \right) \quad (5)$$

$$f_{CD} = \frac{1}{2} f_{rm} \left( 1 - \frac{BD}{PD} \cos \phi \right) \quad (6)$$

where  $f_{rm}$  is the rotor speed in revolutions per minute; others parameters are relate to the geometry of ball bearing and is shown in figure 1: Vibration analysis has the advantage that its

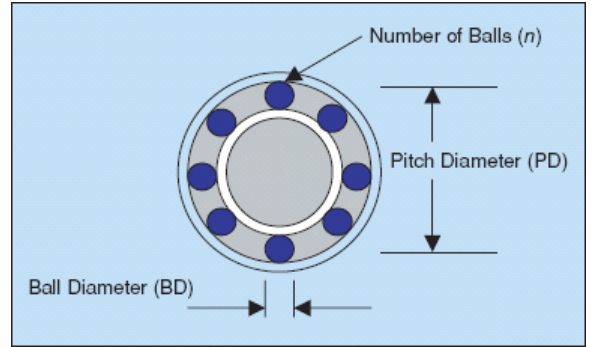


Fig. 1. Bearings parameters [6]

results are independent of the type of motor power supply, high reliability, low power consumption, low cost and yields good results, but its implementation requires using accelerometers as the basic sensors that must be placed near or on the motor; the sensor is exposed to a possible bad environments, this reduce the lifespan of the sensor and its reliability.

### III. METHODOLOGY

The project use an experimental setup composed by a vibration simulator (Dylab mvs 510) and a Texas instrument industrial radar, the AWR1843 single-chip with a frequency range from 76[GHz] to 81[GHz]. As shown in figure 3, the vibration simulator, is composed by an Siemens 2 pole induction motor(IM) characterised by a rated speed of 1670[rpm] with a rated maximum power of 0.37[kW]. It is controlled by a variable frequency driver (VFD) which allows to set the electrical supplying current frequency  $a$  of the motor in order to regulate the speed. The electrical supplying frequency is double the mechanical frequency of the shaft,  $f_{electrical} = 2f_{shaft}$  (a better explanation in the appendix). The motor drives the main shaft which is supported by 2 main bearings (elements n.4 in figure 3). In order to simulate the vibration the system is equipped with known defected bearings: one has a 1mm inner race hole, the second bearing has a 1mm outer race hole. The bearings has specific parameters:

- Bd:ball diameter=7.95mm
- Pd: pitch diameter=33.53mm
- Nb: number of balls =8

In each support there are 3 slots for each support, the bearing in the central position is working, the other on the side aren't connect to the shaft; this construction helps to exchange easily between faulty bearing and normal one to simulate all different cases. The shaft is also connected, through a reduction gearbox, to a magnetic brake (element n.3 in figure 3); an higher load on the system increase the vibration due to the higher torque applied by the motor if a bearings is defective, but it generates also vibrational noise because the gear coupling isn't perfect, this affects the readings. The right end of the shaft is used as target for the radar because it oscillates more than the left end which is closer to the motor and is better for a radar which hasn't an high range resolution (approx. 1 mm).

The start-up procedure of the simulator require, after connect-



Fig. 2. VFD control panel

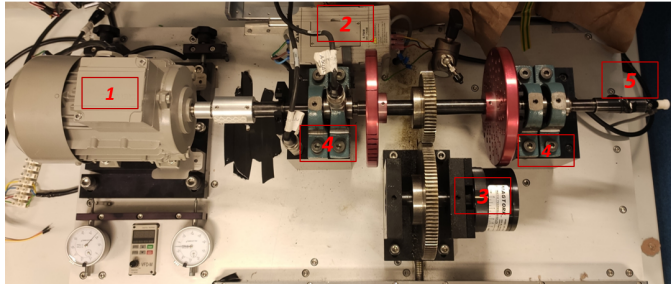


Fig. 3. Vibration simulator DyLAB MVS-510: (1)IM, (2)VFD, (3)Magnetic load, (4)Bearings, (5)radar target

ing it to the power supply, to press the button for powering which active the VFD. Once done that the control panel turns on and is possible to set the rotational speed. The VFD can generate different type of signal: acceleration and deceleration ramp, a step frequency signal and so on. The project's aim is to detect vibrations at steady state so a step frequency signal is applied to the motor. In order to change the frequency applied to the motor is necessary to press the button "mode" on the control panel until a letter "F" appear on the monitor (as shown in figure 2); this means that is possible to control directly the supplying frequency.

Through the knob on the VFD panel is possible to set the supplying frequency that corresponds at double of the rotational frequency of the shaft (better explanation on appendix). After this procedure is necessary to press the button "motor run/stop" for powering the motor and boot it. For safety reasons the motor doesn't start if the coverage is open; in order to bypass this safety measure an electrical switch located behind the motor must be pressed for the entire run period. To improve the quality of the radar's readings the background and most of the reflective parts are covered (as shown in figure 13). The measurements are affected by the reflection of the radio waves from shiny objects; to reduce the reflection has been used cardboard to cover the background, turned off the lights and reduced the field of view of the lidar forcing it to point straight to the target using bulkheads.

In order to acquire the vibration data a Texas Instrument industrial radar, the AWR1843 single-chip is used. This radar is a CWFM one (continuous wave frequency modulation) based on mmW (millimeter wave) technology that uses short-wavelength electromagnetic waves so in the millimetre range; this means working in a frequency range of 30-300 GHz. It

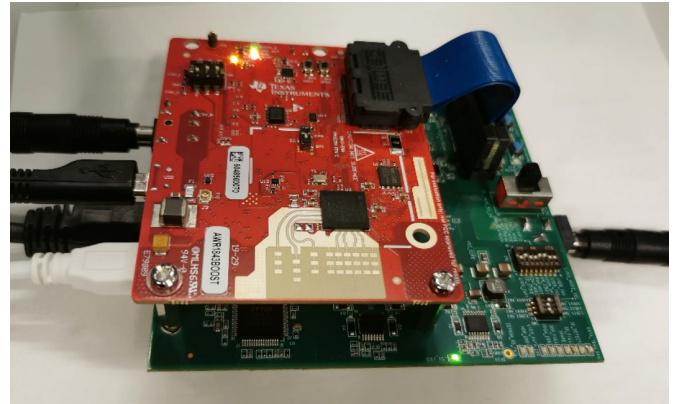


Fig. 4. Radar and acquisition card connected

is based on the fundamental concept of the transmission of an electromagnetic signal, which interferes with an object in its path and then gets reflected back. The electromagnetic signal sent by the radar is called *chirp*, generated by synthesizer, it is a sinusoid whose frequency increases linearly with time. A transmitter antenna (TX ant) emits the chirp, and the reflection of this chirp gets captured by the receive antenna (RX ant). These 2 signals get combined in a "mixer", to produce an intermediate frequency (IF) signal. If there are multiple objects in front of the radar, the IF signal then consists of multiple tones, and each tone is proportional to the range of each object. This signal then gets digitized, and an FFT (fast Fourier transform) is performed on it. In the resulting frequency signal, called range FFT, the location of the peaks corresponds to the range of the objects. The relationship between the range of an object and the frequency in the FFT range signal is:

$$f_{IF} = \frac{2Sd}{c} \quad (7)$$

where  $c$  is the speed of light ( $3 \times 10^8 [m/s]$ ),  $S$  is the slope of the frequency modulation of the chirp and  $d$  is the distance from the object. The radar is characterised by a range resolution calculated as:

$$d_{min} = \frac{c}{2B} \quad (8)$$

$B$  is the working bandwidth of the chirp. The radar can also measure the velocity of an object with further processing of the range FFT signal. Each signal in the frequency domain is complex so it has a phase and an amplitude. If an object is moving, transmitting two chirps separated by a short delay  $T_c$ , the final range-FFTs signal corresponding to each chirp will have peaks in the same location but with differing phase. The phase difference  $\Delta\Phi$  between two signals is related to a motion of the object; so its speed can be calculated:

$$v = \frac{\lambda\Delta\Phi}{4\pi T_c} \quad (9)$$

where  $\lambda$  is the wavelength.

The experimental setup used in this project requires that to acquire data and set parameters, the radar is used with the acquisition card, DCA1000EVM which enables the user access to the sensor's raw data over Ethernet. The entire setup requires

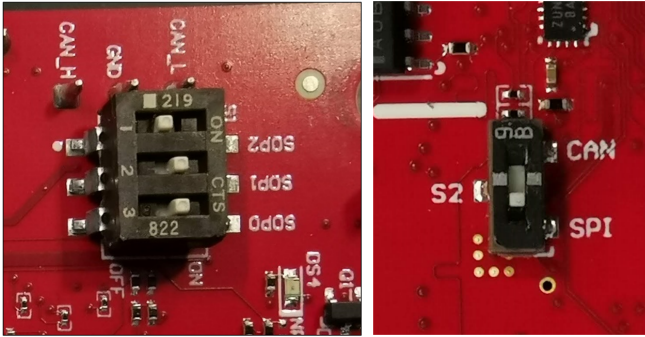


Fig. 5. Radar switches configuration

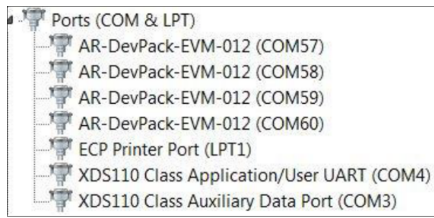


Fig. 6. Ports configuration

2 power supply with at least 2.5[A] with barrel connector (2.1[mm]) one for each board and for the radar itself a micro-usb cable is used to connect it to a laptop. The acquisition card requires micro-USB cable and RJ45 Ethernet cable to connect it to the laptop and a 60pin Samtec cable which connect this board to the radar, shown in figure 4. To use the AWR1843 with mmWave Studio software, the SOP mode needs to be set to development mode (mode 2) on the board obtainable with the switches configuration shown in 5. It also enables the connection to the board via SPI (Serial Communication Protocol). For the two COM ports of the AWR1843 (in figure 6: COM4 and COM3), the driver should already be installed. The FTDI device ports of the DCA1000 board however won't be available because their driver is not installed. The driver for these ports can be found in the mmWave Studio folder. Then the ethernet cable of the DCA1000 must be connected to the computer and in the local area network properties a static IPv4 address of 192.168.33.30 and a subnet mask of 255.255.255.0 need to be set. This settings enables the communication between the board and the laptop through Ethernet.

The software used for acquiring data is mmWaveStudio which, after its execution from the installation location, the FTDI Connectivity Status as indicated with 1 in figure 8 should be highlighted in green and set to "Connected" the following steps need to be executed in order, as shown in figure 7:

- 1) Ensure that DCA1000 is selected.
- 2) Press "Set" in Reset control.
- 3) Select the right COM port number based on figure 6 and a Baud Rate of 115200 and connect.
- 4) Load the appropriate BSS (radarsss.bin).
- 5) Load MSS firmware (Masterss.bin); The binary is based on the device variant being used (1243/1443/1642) and the silicon PG version being used (ES1.0, ES2.0, ES3.0).

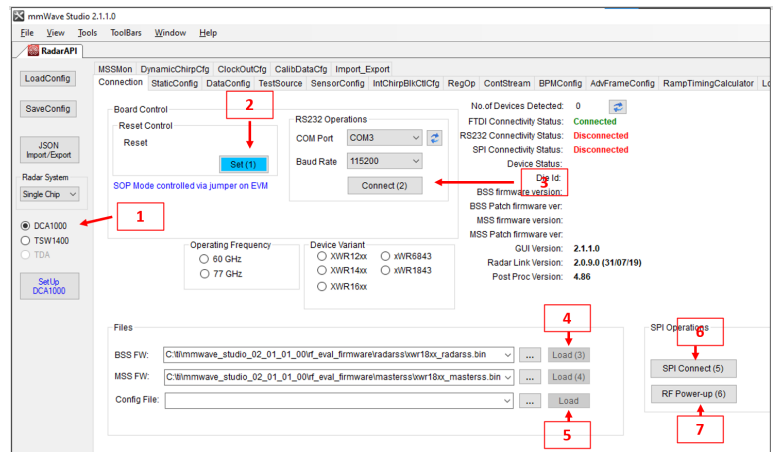


Fig. 7. set up process in mmWaveStudio[part 1]

No.of Devices Detected: 1  
FTDI Connectivity Status: Connected  
RS232 Connectivity Status: Connected  
SPI Connectivity Status: Connected  
Device Status: XWR1642/ASIL-B/SOP2:ES:2  
Die Id: Lot:7541000/Wafer:1/DevX:1/DevY:18  
BSS firmware version: 2.0.0.1 (05/10/17)  
BSS Patch firmware ver: 1.1.0.2 (10/04/18)  
MSS firmware version: 1.0.18.13 (23/03/18)  
MSS Patch firmware ver: NA  
GUI Version: 2.1.1.0  
Radar Link Version: 2.0.9.0 (31/07/19)  
Post Proc Version: 4.86

Fig. 8. connection status in mmWaveStudio

- 6) Click the SPI Connect button.
- 7) Click the RF Power up button.

at the end of this procedure in the software must be shown that all connection are enabled as shown in fig. 8. Then, changing to the *Radar Studio Static Config* tab, the following steps need to be run:

- 1) Select the desired TX and RX channels,in ADC Config select the desired AD configuration and click *Set*.
- 2) Click the *Set* button in the Advanced Configuration box.
- 3) In the LP mode box select *Regular ADC*.
- 4) Press *RF Init Done* button.

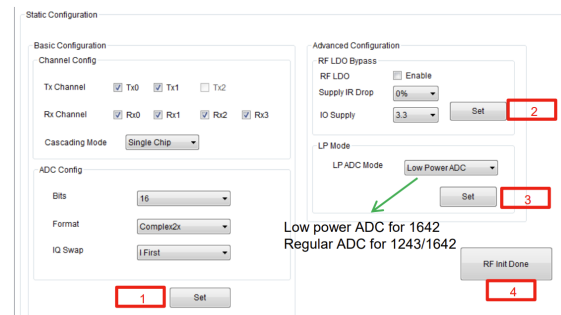


Fig. 9. set up process in mmWaveStudio [part 2]

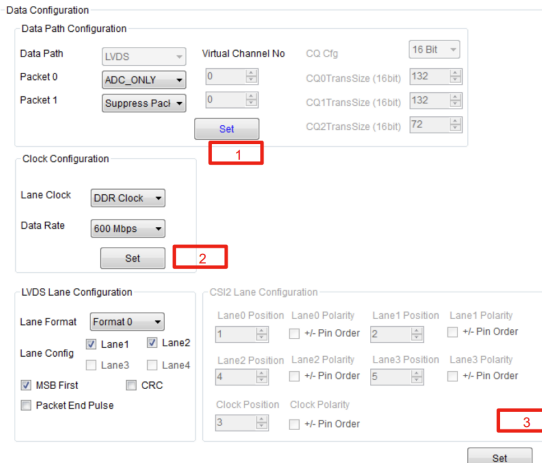


Fig. 10. set up process in mmWaveStudio [part 3]

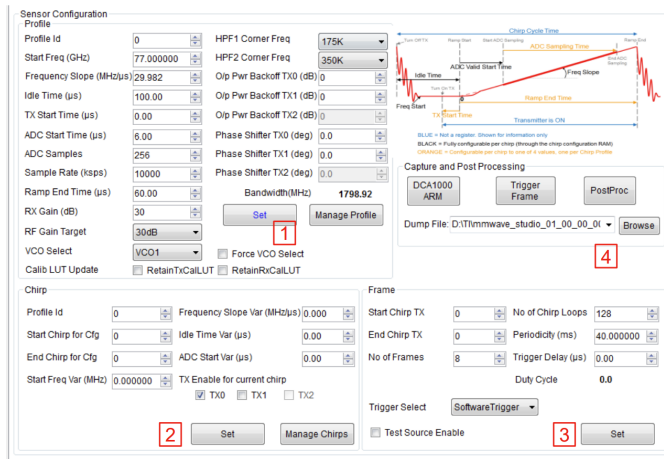


Fig. 11. set up process in mmWaveStudio [part 4]

Moving to the *DataConfig* tab this steps has been done(also shown in figure 10):

- 1) Clic *Set* button in the "data path config" box.
- 2) Choose a 600[Mbps] clock rate and click .
- 3) Select the 4 LVDS lanes and click *Set*.

After, the following steps in the *SensorConfig* tab has been done(explain in fig. 11) :

- 1) Define the FMCW chirp profile and click *Set*.
- 2) Select the chirp configuration and click *Set*.
- 3) Select the frame configuration and click *Set*.
- 4) Select the Dump file pathname in which the radar data will be saved and click *Set*.

As final configuration clicking in the button *setUp DCA1000* on the left side of the panel a new window pops up and clicking on *Connect, Reset and configure* it would establish the Ethernet connection and display the FPGA versions. After all this steps the radar is ready and to start the acquisition process and save into a binary file the range data, is necessary to press in order the buttons: *DCA1000 ARM*, *Trigger Frame* and *Post Proc* (see figure 12).

The radar is placed at 60[cm] from the right end of the shaft and its field of view is perpendicular.

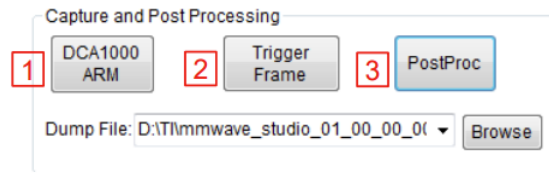


Fig. 12. set up process in mmWaveStudio [part 5]

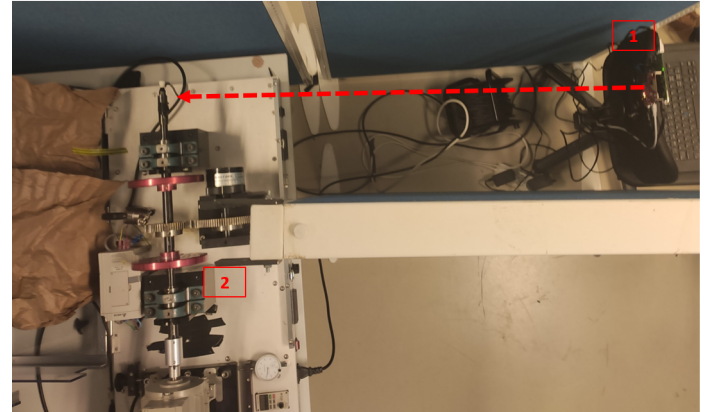


Fig. 13. Experimental setup with the radar (1) and a vibration simulator (2).

The experiment is divided into 4 main sections: at first will be measured the distance of the shaft in stationary condition obtaining the ground truth for the following measurements. Then will be measured the distance of the target while the motor is running with healthy bearings at 5,15 and 25[Hz] and then the measurements are repeated but with faulty bearings, a inner race defect has been chosen. The maximum frequency of 25[Hz] has been chosen in order to have a safety threshold from the maximum frequency of 30[Hz]. For each condition, the range over the entire measurement period plot and the Doppler plot is being compared to analyse the performance of the radar. The data obtained with the radar, saved in a binary file, are being processed using a specific Matlab code in order to compare the SDK plots with the Matlab post-processed plots. In the end, to validate the possibility to measure the rotational speed of the shaft using a radar it was located under the shaft where a piece of reflective tape was located, as shown in figure 14.

#### IV. GRAPHICS AND MEASUREMENTS

In order to set a ground truth for the vibration analysis, have been measured the distance of the shaft in stationary condition, so with the motor off. In this situation, comparing the SDK range plot and the Matlab plot,figure 15, is noticeable that the results are the same but with a different scaling in the y-axis; in the Matlab plot the first peak can be associated to the shaft, so the measured distance is 0.78[m] from the radar instead of 0.6[m] and the higher peak at measured 1.37[m] is related to the background which is in reality at approximately 1.2[m]. The Doppler plot, figure 16, confirms that everything is stationary because there is only a yellow line centred at 0[m/s], means that all the detected object are static. If there is something

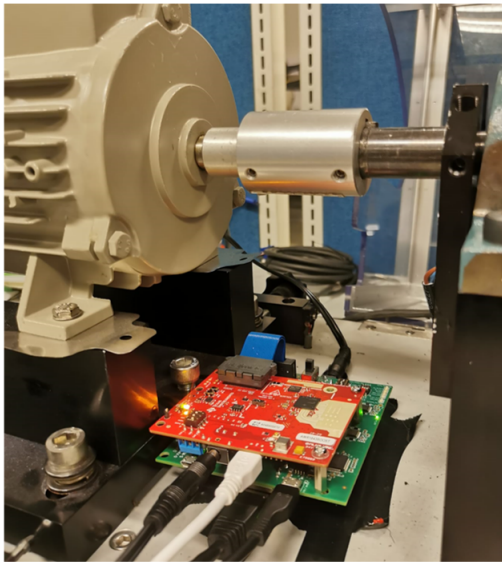


Fig. 14. setup for rotational speed measurements

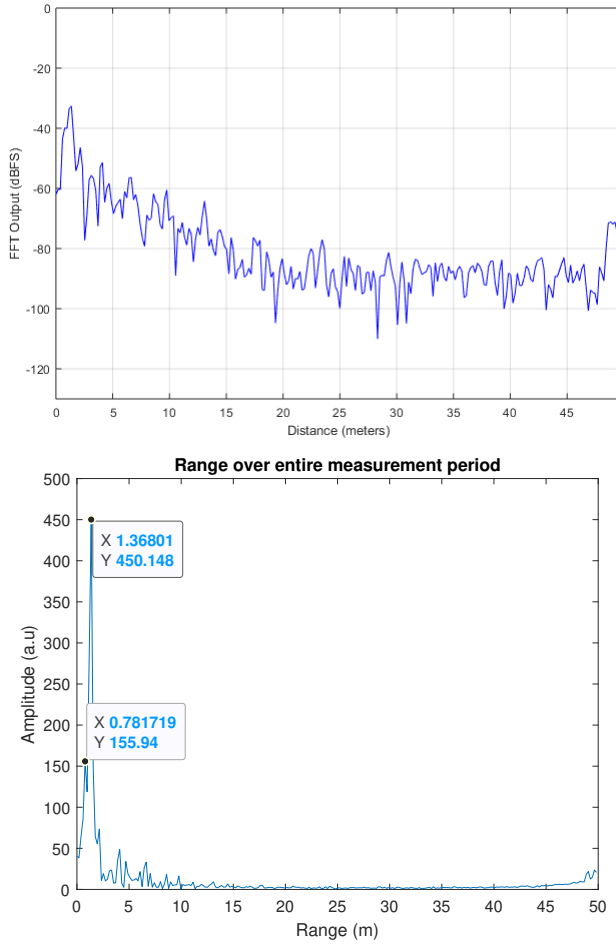


Fig. 15. stationary condition; top: SDK range plot; bottom: Matlab range plot

moving, should appears some yellow line at the measured speed.

Turning the motor on and setting the rotational frequency of the shaft to 5[Hz], it means setting a frequency of 10[Hz]

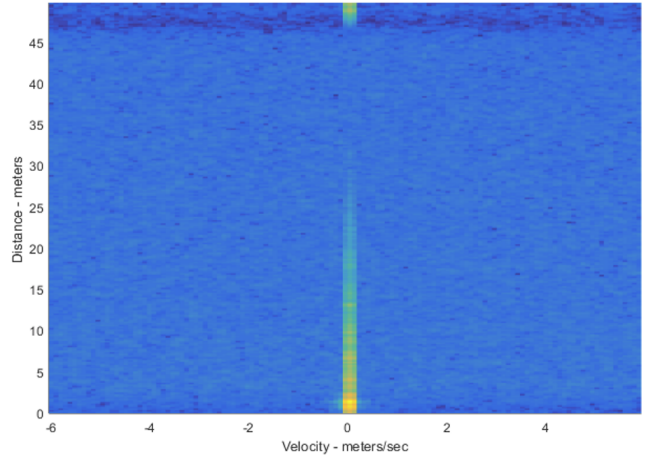


Fig. 16. Doppler plot in stationary condition

on the VFD control panel, can be notice that the in the figure 17 there are no peak related to the shaft it is included into the second peak located at 1.36[m]. But, from the Doppler map, figure 18, can be noticed that there is a yellow halo around 0[m/s], which can be associated to noise but also to some slow vibration of the system caused by the load and by a possible misalignment between the motor and the shaft.

Increasing the frequency to 15[Hz] the range plot (figure 19) doesn't change compared with the one at lower frequency but from the Doppler plot, figure 20, the yellow halo is spread in a larger section, means that the noise depends from the rotational frequency and the radar is capturing movement caused by miss alignment and other moving parts.

The last frequency tested with healthy bearings is 25[Hz] which confirm the theory that the noise is related to the rotational frequency, in fact the yellow halo in figure 22 is better spread across all the speed range.

Adding the faulty bearing, in particular the inner race defected one, and setting the rotational frequency again to 5[Hz] from figure 23 is noticeable a peak at 0.58[m] caused by the movement of the shaft thanks to the faulty bearing. From the doppler plot, figure 24 , in the boxed area can be noticed 4 peaks (more intense yellow zone) at low speed at the shaft range approximately.

Increasing the frequency to 25[Hz] and processing the data is noticeable that in figure 25 the first peak is related to the shaft but it has a double tip as describing the vibration of the shaft. From the heat map, figure 26, is clear that the radar is detecting the shaft moving at a speed of approximately  $\pm 2.8[m/s]$  and  $\pm 3.5[m/s]$ . These speed values can be related to the first two harmonics of the shaft displacement.

The last experiment is with a frequency of 25[Hz]; in this case from the range FFT plot there is only one spike in the shaft-range, this could be related to a not high resolution of the radar because at higher frequency the vibration become

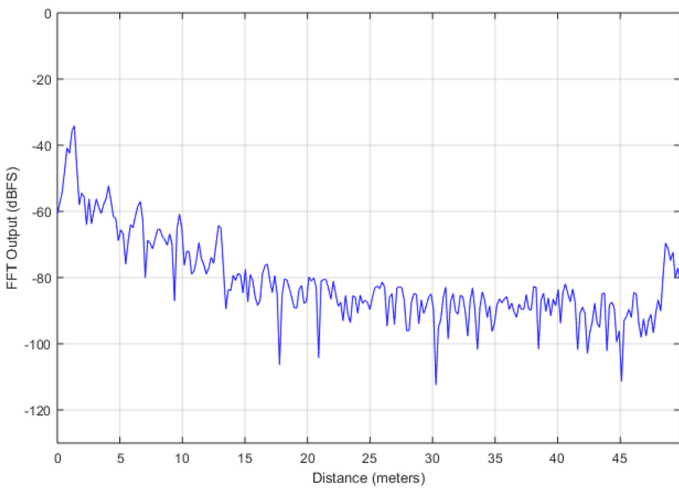


Fig. 17. healthy bearings at 5[Hz]; top: SDK range plot; bottom: Matlab range plot

faster and the intensity of the reflected waves is lower. But, looking at the Doppler plot the radar detects the 2 main harmonics at an higher frequency than the previous case with 15[Hz].

Plotting all the already shown result in the same graph, figure 29, is clear that in all conditions the radar detect the presence of the shaft but only at lower frequency 5[Hz] and 15[Hz] (green and light blue line) the first peak as a more flatten tip. The flatten tip is caused by the change in displacement of the shaft due to the fault.

## V. CONCLUSION AND DISCUSSION

This paper shows that it is possible to implement a radar for detecting a vibration of a motor shaft caused by a faulty bearing instead of using a contact sensor like in the vibration analysis; overcoming the drawbacks of this common-used method, in particular it can solve some problems related to the use of contact sensor, such as accelerometers, which they have reduced lifespan if they are forced to work in a hostile environment and they require to be in contact with the object. Determine the continuous health status of a motor can help to

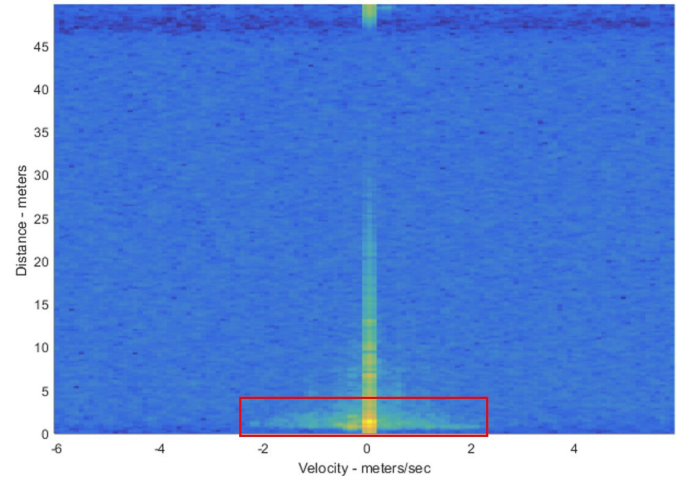


Fig. 18. Doppler plot with healthy bearings at 5[Hz]

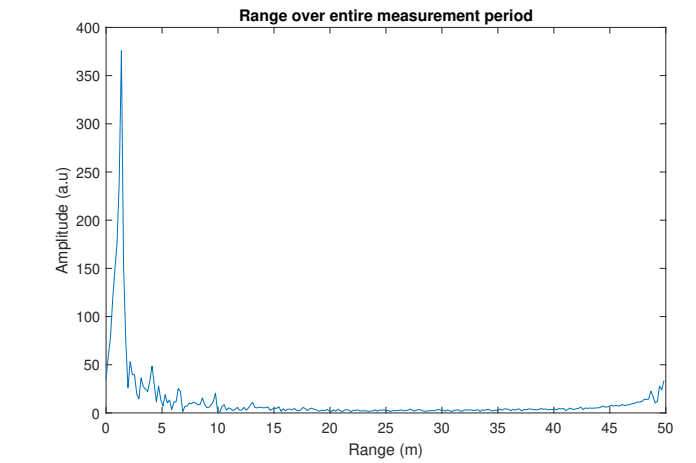
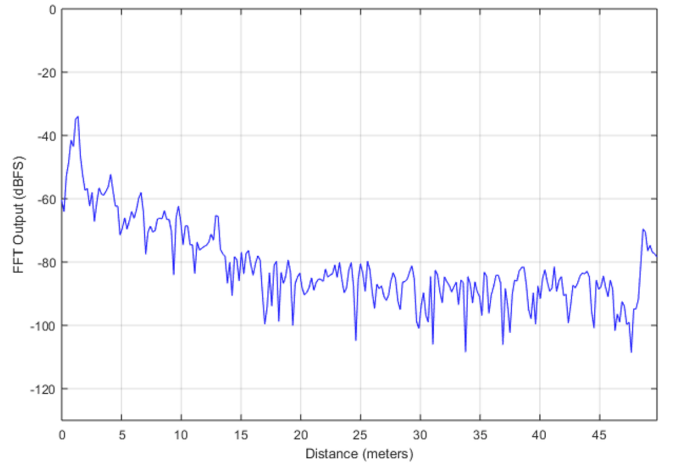


Fig. 19. healthy bearings at 15[Hz]; top: SDK range plot; bottom: Matlab range plot

develop different type of predictive maintenance. For example, it is possible to determine if some components inside of the motor are going to fail and schedule a maintenance before the break; this helps reducing drastically the downtime of a machine.

Has been demonstrated that a radar is able to detect the

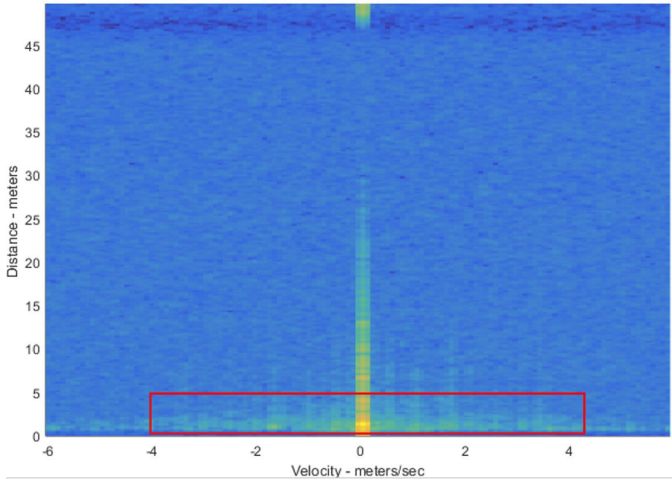


Fig. 20. Doppler plot with healthy bearings at 15[Hz]

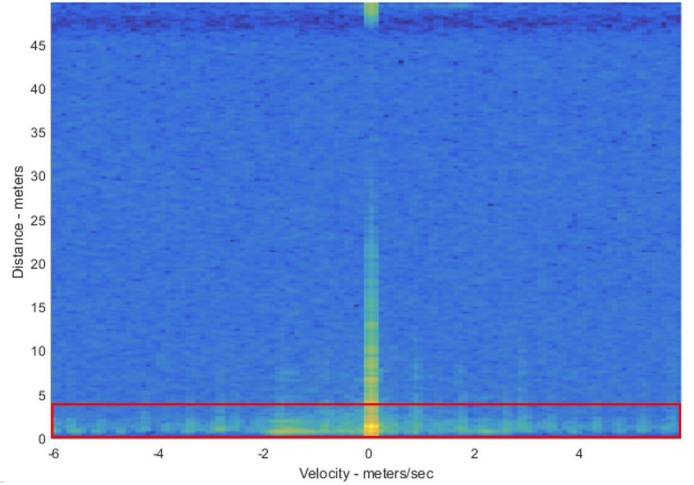


Fig. 22. Doppler plot with healthy bearings at 25[Hz]

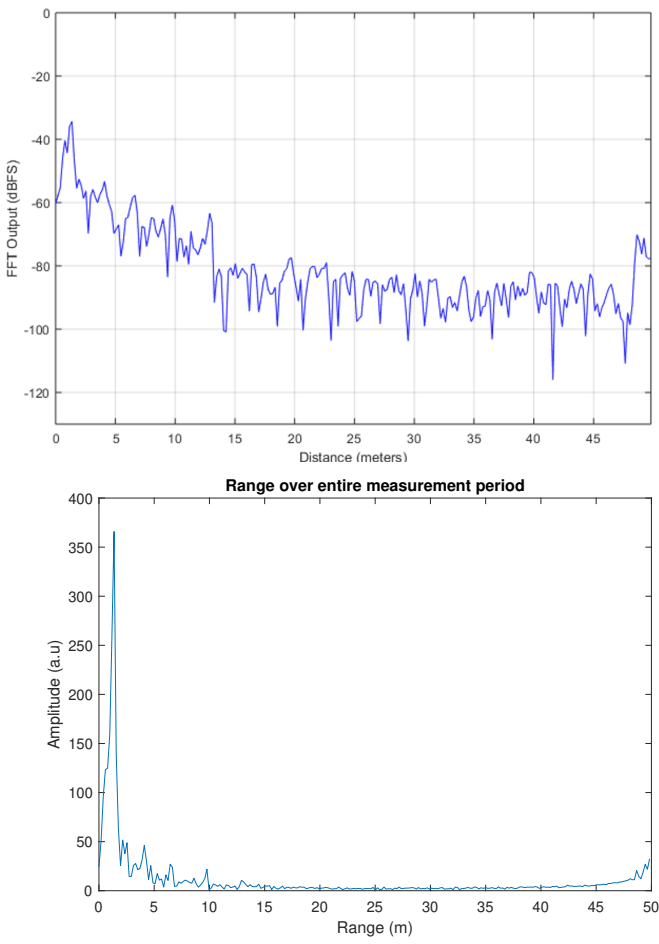


Fig. 21. healthy bearings at 25[Hz]; top: SDK range plot; bottom: Matlab range plot

position of a shaft and its vibration at low frequency, in fact referring to figure 29, with faulty bearings at 15 [Hz] and 5[Hz] the first peak in the range fft plot has a flatten tip, this means that the radar detected the changing displacement of the shaft (vibration), this is also visible from the Doppler plot

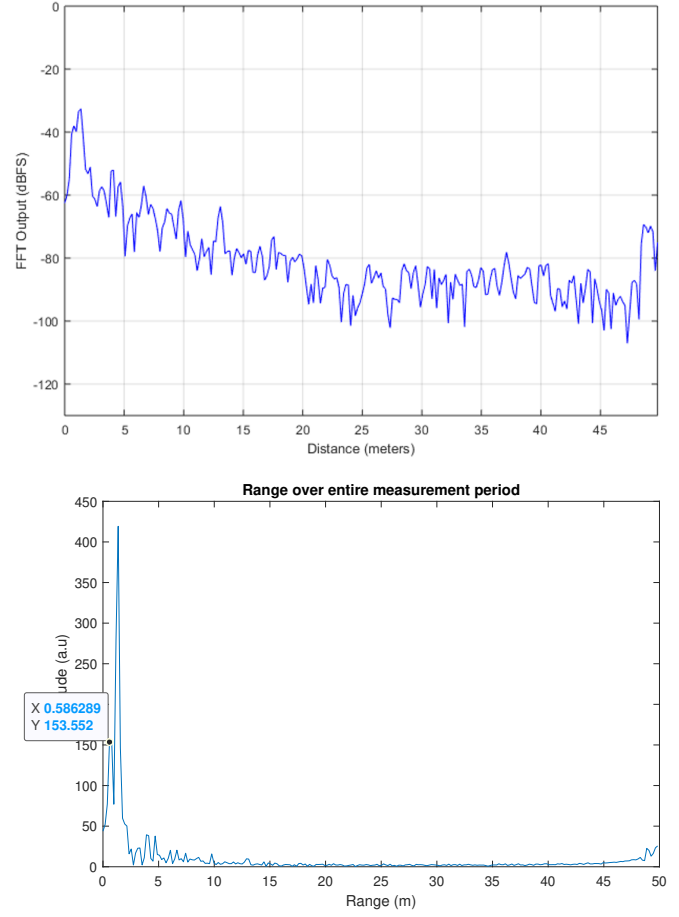


Fig. 23. faulty bearings at 5[Hz]; top: SDK range plot; bottom: Matlab range plot

where, as indicated by the arrows, there are 4 areas with higher intensity that are symmetrical respect to the center (0 value), this is related to the ability of the radar to detect only the first and the second harmonics of the vibration of the shaft; increasing the rotational frequency these higher intensity spots pull away from the zero, confirming that these spots show to

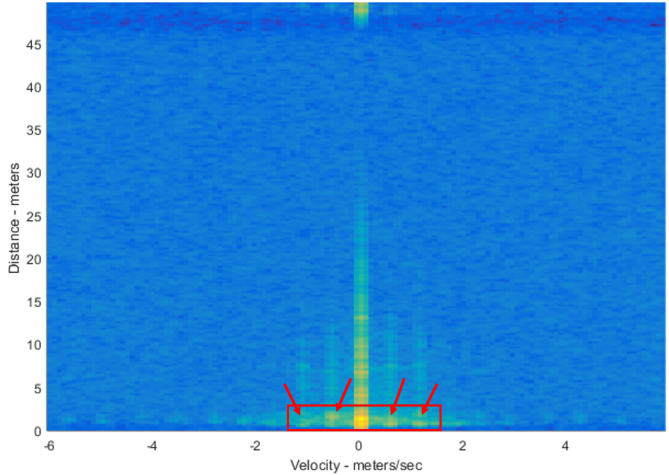


Fig. 24. Doppler plot with faulty bearings at 5[Hz]

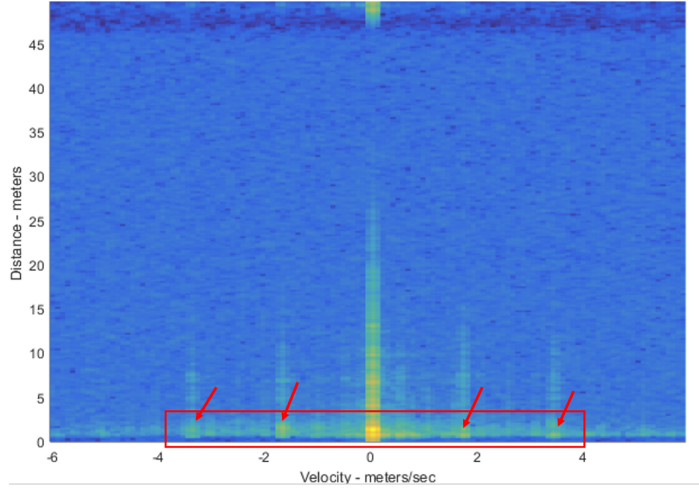


Fig. 26. Doppler plot with faulty bearings at 15[Hz]

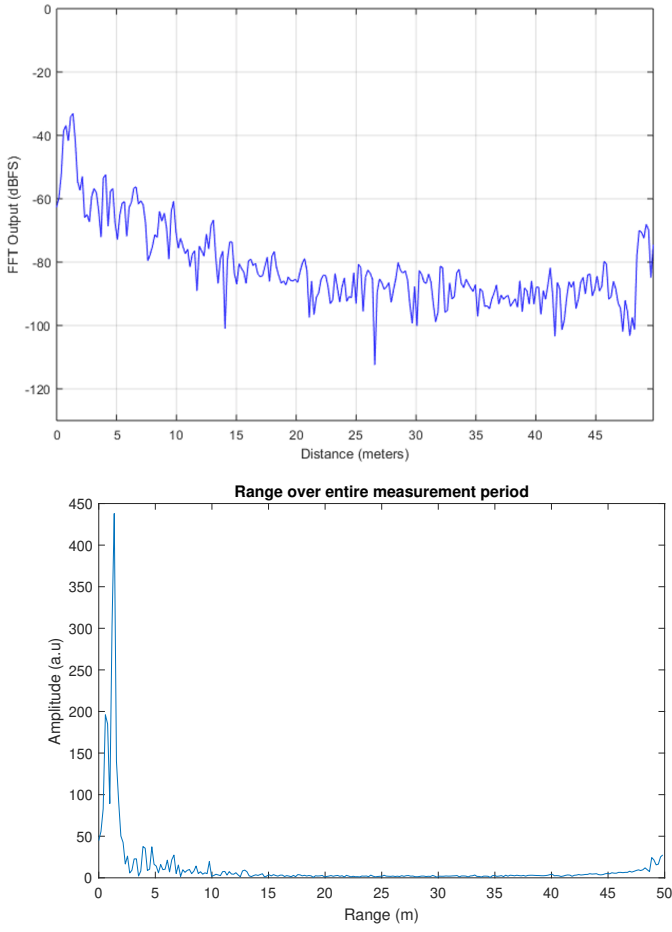


Fig. 25. faulty bearings at 15[Hz]; top: SDK range plot; bottom: Matlab range plot

the first and second harmonics of the vibration signal. Also in this case, at lower frequency these areas are more recognisable for multiple reasons; the first reason and the most relevant is the radar's resolution: the radar as limited range resolution and speed resolution this limits the possibility to detect very small and rapid changes of the shaft's position. Another key

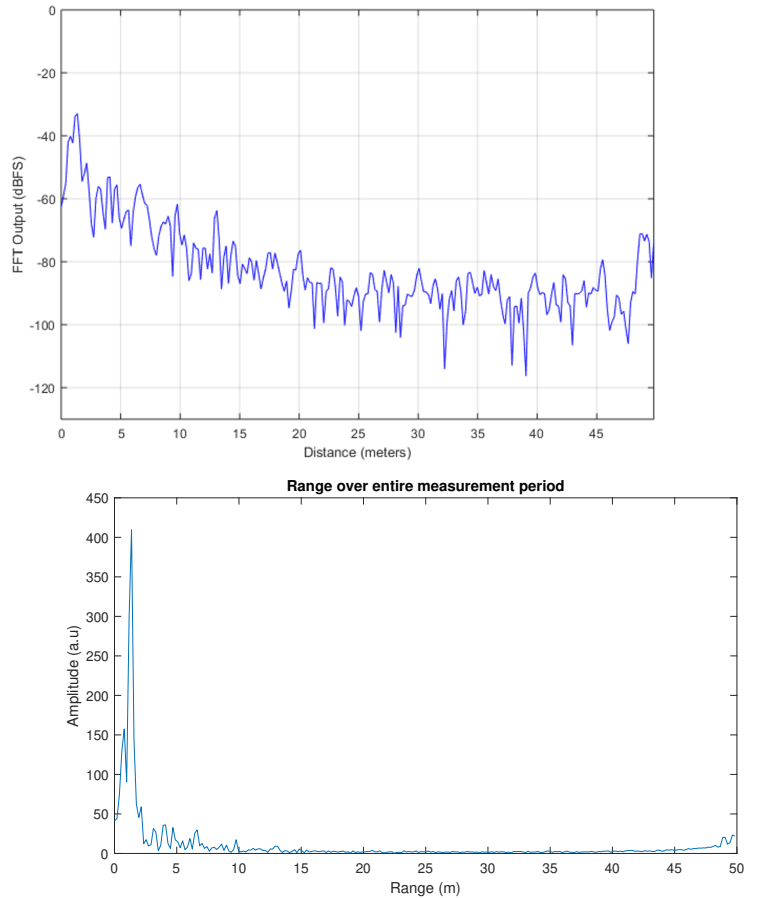


Fig. 27. faulty bearings at 25[Hz]; top: SDK range plot; bottom: Matlab range plot

factor is the measurement noise, comparing the range ff plot at the same rotational frequency but with healthy and faulty bearings (example figure 18 and figure 24) there is a lot of background noise that interferes with the acquisition: this noise can be generated by the reflection of other components of the experimental setup with the radar, because not only the shaft is rotating but also the gearbox and the flywheel of the system,

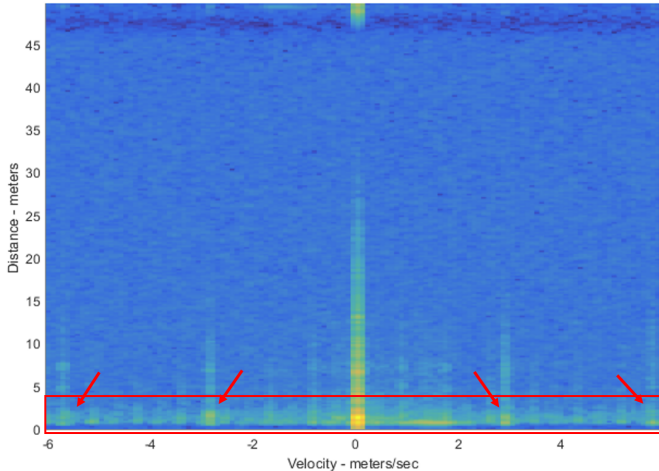


Fig. 28. Doppler plot with faulty bearings at 25[Hz]

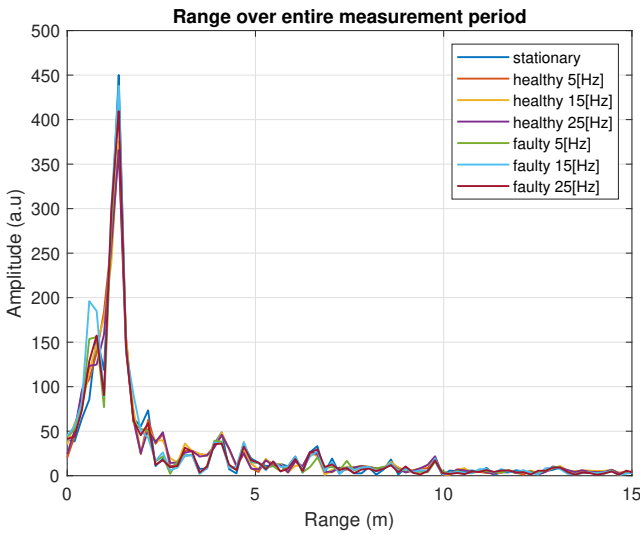


Fig. 29. Range plot of all analysed condition

but also the radar is designed to detect object in a wide area not a range of a single point. Looking at the Doppler plot with healthy bearings (from figure 18 to figure 22) is noticeable that the shaft it is not rotating perfectly, it has some vibration caused by a non perfect alignment of the main shaft with the motor's rotor and also considering that the measurements are taken at the right end of the shaft so it can be prone to bending due to its length.

In conclusion, this paper demonstrate the possibility to determine the vibration of the motor's shaft using a radar, a non contact sensor, but it works better at lower rotational frequency. At higher frequency a lidar, which has an higher resolution, can be more effective for vibration detection.

quest rumore puo essere anche notato guardano il grafico con la scal logaritmica dove ad alta frequenze il rumore è persistente.

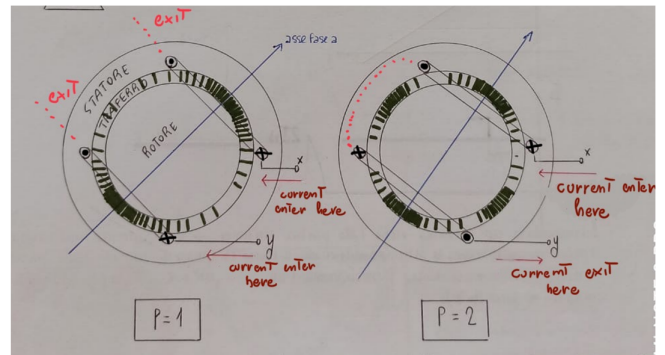


Fig. 30. schematic of induction motor rotor with 1 and 2 polar couples

## APPENDIX A INDUCTION MOTORS

An induction motor, or asynchronous motors, is the most common motor used in industrial application thanks to its reliability and robustness. The electro-mechanical conversion that they carry out follows the principle of operation of induction systems by means of a direct application of the rotating magnetic field. The torque and speed of the motor are strictly dependent to the voltage/current applied to the motor and to its internal structure. Considering a squirrel cage induction motor, a very relevant parameter that affect the mechanical characteristics of the motor is the number of polar couples: higher the number of polar couple lower is the maximum rated speed and higher the torque. As shown in figure 30, the number of polar couples defines the number of magnetic induction peaks in the air gap between the rotor and the stator, and the magnetic induction is responsible for generating the torque in a induction motor. The relation between the rotational speed of the rotor and the supplying voltage frequency is:

$$\omega = \frac{60 f_{\text{supply}}}{p} \quad [\text{rpm}] \quad (10)$$

where  $p$  is the number of polar couples,  $\omega$  the speed of the shaft in rpm and  $f_{\text{supply}}$  is the frequency of the voltage which supply the motor. In this project to determine the rotational speed of the shaft with a 2 polar couple motor, is necessary to divide by 2 the frequency set by the VFD.

## APPENDIX B VIBRATION ANALYSIS WITH A LIDAR

Another possibility to improve the vibration analysis technique is to use a lidar instead of a radar. This type of sensor has a higher range resolution thanks to the higher working frequency of the laser. In order to set up a Lidar, multiple steps must be followed, the steps are explained to connect a SICK LMS133 2D lidar Nvidia jetson nano. To detect the shaft's vibration a 2D lidar is used and it is positioned perpendicular to the shaft, otherwise a misalignment in the Lidar cause a mis-reading of the shaft's displacement. The position's data produced by the lidar are sent to a computer unit through a Ethernet cable. The choice of the jetson nano is due to the necessity of more computational power than a raspberrypi, because the aim is to process data in almost real time with

complex algorithms. On the board is installed Ubuntu 18.04 with ROS 1 melodic version, this is the only ROS version suitable for this type of Ubuntu. The Lidar used in this project is the LMS133, made by SICK, it has an aperture angle of 270° horizontal with a frequency of 50/25 [Hz], and a very large range of detection (20 [m]), as default. It communicates with the board through a Ethernet cable, so its necessary to set properly the ip-addresses of the board and the Lidar. The ip of the lidar must have the same value of the board ip for every number that is covered by the subnet-mask but they have to differ in the other numbers; in this case the Lidar's ip is 192.168.0.1 (it's the default value), so the board's ip must be 192.168.0.x (because the subnet-mask is 255.255.255.0) where x could be every integer number different from 1. To set properly the IPs is possible to change the Lidar's ip through the manufacturer's proprietary software, SOPAS Engineering Tool (available only for Windows OS), or to change the board's ip from the settings. Once connected the Ethernet cable to the board in order to set up the communication is necessary to remove the *docker0* interface that is pre-installed in OS such as Ubuntu for jetson; to do that must be run the command: *sudo ip link delete docker0*. This interface is a virtual bridge created by Docker; it randomly chooses an address and subnet from a private defined range and it assigned to the device, to guarantee a better safety of the board. It's possible to check the presence of *docker0* using the command *ipconfig*, which shows all active interfaces on the board. Whereupon, through the manufacturer github repository, is necessary to download and install the open-source project to support the laser scanner for ROS 1, that is called *sick scan*. This stack provides a ROS driver for multiple SICK lidar and radar sensors. Following the guided procedure for the download, recommended from source, adding also the development branch for more update support for all the Sick lidar. Summarising the mandatory commands:

- 1) *source /opt/ros/melodic/setup.bash*
- 2) *mkdir -p /ros\_catkin\_ws/src/*
- 3) *git clone git://github.com/SICKAG/sick\_scan.git*
- 4) *cd ..*
- 5) *catkin\_make install*
- 6) *source /ros\_catkin\_ws/install/setup.bash*

Then all the steps must be repeated to install the development branch but at step 3 the command is : *git clone -b devel-single-branch git://github.com/SICKAG/sick\_scan.git*. The command at step 6 must be run every time is necessary to open a new terminal and working with lidar commands/data. To change Lidars's parameters like for example: maximum and minimum angle of scanning, type of data, intensity etc is necessary to modify the launch file before the start of the ROS node. The launch file, of the specific lidar that we are going to use, is contained in the source folder (*src*) of the local ROS repository folder (usually called "*catkin-ws*"). After setting all the parameters the ROS node is launched to start acquire data from the lidar which are published on the topic *pointcloud2* through the command *roslaunch sick\_scan sick\_lms\_1xx*.

## APPENDIX C GITHUB REPOSITORIES

- Project repository: [https://github.com/gianlucasalata-unipd/MASS13-Continuous\\_motors\\_health\\_monitoring](https://github.com/gianlucasalata-unipd/MASS13-Continuous_motors_health_monitoring).
- Lidar repository: [https://github.com/SICKAG/sick\\_scan](https://github.com/SICKAG/sick_scan)

## REFERENCES

- [1] Paulo Antonio Delgado-Arredondo, Daniel Morinigo-Sotelo, Roque Alfredo Osornio-Rios, Juan Gabriel Avina-Cervantes, Horacio Rostro-Gonzalez, Rene de Jesus Romero-Troncoso, Methodology for fault detection in induction motors via sound and vibration signals, Mechanical Systems and Signal Processing, Volume 83,2017,Pages 568-589,ISSN 0888-3270,
- [2] Kim Dong-Yeon, Yun Han-Bit, Yang Sung-Mo, Kim Won-Tae, Hong Dong-Pyo, Fault Diagnosis of Ball Bearings within Rotational Machines Using the Infrared Thermography Method, Journal of the Korean Society for Nondestructive Testing / v.30, no.6, 2010 , pp. 558-563
- [3] J. Jung, J. Lee and B. Kwon, "Online Diagnosis of Induction Motors Using MCSA," in IEEE Transactions on Industrial Electronics, vol. 53, no. 6, pp. 1842-1852, Dec. 2006, doi: 10.1109/TIE.2006.885131.
- [4] R. R. Schoen, T. G. Haberler, F. Kamran and R. G. Bartfield, "Motor bearing damage detection using stator current monitoring," in IEEE Transactions on Industry Applications, vol. 31, no. 6, pp. 1274-1279, Nov.-Dec. 1995, doi: 10.1109/28.475697
- [5] W. T. Thomson and M. Fenger, "Current signature analysis to detect induction motor faults," in IEEE Industry Applications Magazine, vol. 7, no. 4, pp. 26-34, July-Aug. 2001, doi: 10.1109/2943.930988.
- [6] M. J. Devaney and L. Eren, "Detecting motor bearing faults," in IEEE Instrumentation & Measurement Magazine, vol. 7, no. 4, pp. 30-50, Dec. 2004, doi: 10.1109/MIM.2004.1383462.